Mutations in the reduced-folate carrier affect protein localization and stability

Heather SADLISH, Richard C. MURRAY, Frederick M. R. WILLIAMS and Wayne F. FLINTOFF[1]

Department of Microbiology and Immunology, University of Western Ontario, London, Ontario, Canada N6A 5C1

The reduced-folate-carrier (*rfc*) gene has been shown to be functionally important for reduced-folate transport in mammalian cells. In the present paper we describe the identification of alterations in both alleles of the *rfc* gene in a mutant Chinese-hamster ovary cell line deficient in methotrexate transport. One allele of the *rfc* gene contains a point mutation resulting in a $Gly^{345} \rightarrow Arg$ substitution in the predicted amino acid sequence. In this case, a protein of similar size to the wild-type protein is produced, although it remains as an immature, core-glycosylated, form. The second allele contains a point mutation in the last base of intron 5 that results in the utilization of a cryptic splice site leading to a seven-base deletion in the mRNA. The use of an alternate splice site changes the reading frame to yield a truncated protein with 68 different C-terminal amino acids as compared with the wild-type. Both of these altered gene products were monitored by fusion with green fluorescent protein and found to be non-functional with an increased rate of turnover. The protein with the point mutation is trapped in the endoplasmic reticulum with subsequent degradation, whereas the product of the splice mutation is not membrane-associated and is partially degraded. Thus mutations in both alleles of the *rfc* gene in this resistant cell line account for the loss of reduced-folate transport. The observations made regarding the degradation of these mutant gene products also provide support for putative checkpoints in the endoplasmic reticulum.

Key words: methotrexate resistance, membrane protein, N-glycosylation, protein degradation.

INTRODUCTION

The reduced-folate-carrier (RFC) transport system is involved in the intracellular accumulation of folates in mammalian cells and has been examined in hamster [1], mouse [2–4], rat [5,6] and human [7,8] systems. RFC transports reduced folates such as methotrexate (Mtx) and folinic acid with relatively high affinity, and folic acid with a low affinity [4]. Reduced-folate transport is essential for normal cell growth and differentiation [9] and is an important determinant of antifolate resistance encountered in chemotherapeutic applications [10]. The cDNAs have been identified from several species [11–19] and the genomic structures for hamster [20], mouse [21,22] and human [23–25] have also been reported. The RFC protein is membrane-localized and correlates with a predicted 12-transmembrane-domain topology [26].

Recent studies have investigated the functional role of the RFC protein through the characterization of altered reduced-folate-carrier (*rfc*) genes, as the study of mutations assists the identification of essential domains in the protein. Point mutations in various locations within the *rfc* coding region have been associated with decreased Mtx transport [27–36]. These have resulted in prematurely truncated proteins [29,30,35], or full-length proteins which are non-functional [27,28], have an altered substrate specificity [31–34] or altered stability [35].

The present study provides the first comprehensive characterization of alterations in both alleles of the *rfc* gene from a mutant Chinese-hamster ovary cell line deficient in Mtx uptake. Both of these mutations are base-pair changes: one in the coding region of the gene and the other at a splice site which leads to a frameshift and premature truncation of the protein. Subsequent characterization of the altered gene products indicated that both changes lead to decreased stability and improper cellular localization. The observations made regarding the degradation of these mutant gene products also provide support for putative checkpoints in the endoplasmic reticulum (ER), which monitors newly synthesized proteins. These results indicate that mutations in both alleles of the *rfc* gene in this Mtx-resistant cell line account for the loss of reduced-folate transport and are consistent with the previous observation that mutations in the *rfc* gene are genetically recessive [37].

EXPERIMENTAL

Reagents

Polybrene was purchased from Sigma. Geneticin (G418) was purchased from Life Technologies Inc. [3′,5′,7′-^{3}H]Mtx (35 Ci/mmol) was purchased from Moravek Biochemicals Inc. (Brea, CA, U.S.A.) and purified by TLC before use as described previously [1]. [α-^{32}P]dCTP (3000 Ci/mmol) and [γ-^{32}P]ATP (6000 Ci/mmol) were purchased from ICN. The pRSET plasmid containing the S65T green fluorescent protein (GFP) sequences was kindly provided by Dr. Roger Y. Tsien (Howard Hughes Medical Institute, University of California – San Diego, San Diego, CA, U.S.A.). pEGFP-N1 was obtained from ClonTech. The brefeldin A–BODIPY™ (4,4-difluoro-4-bora-3a,4a-diaza-*s*-indacene) 558/568 conjugate was obtained from Molecular Probes, Eugene, OR, U.S.A.

Abbreviations used: GFP, green fluorescent protein; EGFP, enhanced GFP; ER, endoplasmic reticulum; Mtx, methotrexate; RFC, reduced-folate carrier; poly(A)$^+$, polyadenylated; RT-, reverse transcriptase; BODIPY™, 4,4-difluoro-4-bora-3a,4a-diaza-*s*-indacene; CFTR, cystic fibrosis transmembrane-regulator.

[1] To whom correspondence and requests for offprints should be sent (e-mail flintoff@julian.uwo.ca).

Cell lines

Clonal cell lines of wild-type Pro$^-$3, mutant Mtx-resistant Pro$^-$3 MtxRII 5-3 (MtxRII 5-3), and Pro$^-$4 MtxRIIOua^R 2-4 (MtxRIIOua^R 2-4) and their maintenance have been previously described [37,38]. The Mtx resistant lines do not transport Mtx. The MtxRIIOua^R 2-4 cells contain *rfc* message, whereas the MtxRII 5-3 cells do not contain detectable *rfc* message when subjected to Northern analysis [11].

Reverse transcriptase-PCR (RT-PCR)

Polyadenylated [poly(A)$^+$] RNA was isolated from $\approx 1.5 \times 10^7$ MtxRIIOua^R 2-4 cells using the QuickPrep Micro mRNA Purification Kit (Pharmacia Biotech Inc.). First-strand cDNA was synthesized from 1 μg of poly(A$^+$) RNA using Superscript II reverse transcriptase (Life Technologies Inc.) according to the conditions recommended by the supplier. Sequences corresponding to the putative coding region of *rfc* were amplified from the first-strand cDNA using forward primer (5′-GTGTTGTAGTGCGCGTGGTG-3′) at bp −221 of the *rfc* cDNA sequence (GenBank® accession no. U03031; [11]) and a reverse primer at bp 1633 (5′-GGAGAGGTTGCTTAAGTCAG -3′) using standard PCR conditions. Immediately prior to PCR amplification, the forward primer was phosphorylated using T_4 polynucleotide kinase according to the conditions outlined in the Eukaryotic TA Cloning Kit-Unidirectional (Invitrogen). The PCR products were purified on a 0.8 %-agarose gel and isolated using the Qiaex II gel extraction kit (Qiagen). The purified PCR products were ligated into the pCR3 unidirectional cloning vector and transformed into TOP 10F' cells according to the conditions of the supplier (Invitrogen). Plasmid DNA was isolated using the RPM Miniprep Kit (Bio 101) and digested with *Hin*dIII restriction endonuclease to determine which mRNA splice variant was represented [20]. Four clones of each of the two splice variants were selected for sequence analysis.

DNA sequencing

Double-stranded DNA sequencing was performed by the dideoxy-chain-termination method using the T_7 Sequencing Kit supplied by Pharmacia Biotech Inc. Sequences were obtained using either T_7 or Sp6 sequencing primers or synthetic oligodeoxynucleotide primers spanning the coding region of the hamster *rfc* gene [11].

Genomic DNA amplification and DNA sequencing

High-molecular-mass genomic DNA was isolated from exponentially growing Pro$^-$3 and MtxRIIOua^R 2-4 cells by the method of Gross-Bellard et al. [39]. Sequences surrounding the two mutations were amplified from 0.1 μg of genomic DNA using primer pairs designed from the hamster *rfc* cDNA sequence [11]. The forward primer (5′-CACGTCCTGTGGAGTATTGA-3′) at position 871 and reverse primer (5′-AGCACGTAGGTCATGTAGAG-3′) at position 1112 span intron 4 of the *rfc* gene and result in a 520 bp fragment after PCR amplification. The second region spanning intron 5 was amplified using a forward primer (5′-GTACATGGTCCACTACGTGA-3′) at position 1050 and a reverse primer (5′-GTCGGAGACCACAAGCGTGA-3′) at position 1260 to yield a fragment of 1950 bp. The PCR products were sequenced directly with the reverse primer used in the amplification with the Amplicycle Sequencing Kit (Perkin–Elmer). In addition, the PCR products were cloned using the pGEM-T vector system (Promega).

DNA transfections

Transfection of the plasmid clones into the recipient MtxRII 5-3 cells was performed using 10 μg of purified DNA in Polybrene/2×10^5 cells as previously described [11]. After transfection with DNA, the cells were selected for growth in either low levels of folinic acid (2 nM) or normal media containing 1.2 mg/ml G418 as previously described [11]. Colonies were picked from individual transfection experiments, cloned by limiting dilution and, if necessary, sorted by FACS to isolate cells expressing the fluorescent enhanced GFP (EGFP). At least two independently generated isolates from separate transfection experiments with each construct were used for analysis. As both isolates for each construct showed similar characteristics, representative data from only one of each type is shown.

For transient transfections, MtxRII 5-3 cells were plated at 1×10^5 cells/well of a 24-well tissue-culture tray and treated with 0.3 μg of DNA/well and LipofectAMINE (Gibco) according to the manufacturer's instructions. At 5 h the transfection was stopped and, at various time points thereafter, cells were monitored for fluorescence or prepared for Western-blot analysis.

Folate uptake

Kinetic analyses for the determination of V_{max} and K_t were carried out as previously described [40].

Construction of GFP fusion proteins

The S65T GFP coding sequences were cloned in-frame to the C-terminal end of the wild-type and both mutant isoforms of the hamster *rfc* gene. The wild-type *rfc* GFP fusion construct was assembled in the pcDNA3 expression vector (Invitrogen) by T. Michael Underhill (University of Western Ontario). The single base-pair change in the pMtxR2-4A-GFP construct was generated by replacing a *Hin*dIII fragment into the wild-type *rfc*–GFP construct.

For the GFP fusion construct with the 7 bp deletion, the novel stop codon was first replaced with a *Bam*HI site using a reverse primer with a 5′ extension (5′-TAGGATCC-ATCCAGCACG-GCCCCG-3′). This primer was used with a forward primer at position 871 to amplify sequences from a clone containing the 7 bp deletion under standard PCR conditions. The resulting PCR product was cloned into the pGEM®-T vector (Promega). A *Bam*HI fragment containing the S65T GFP sequence was cloned into the *Bam*HI site of the PCR product and screened for orientation. From this construct, a *Bpu*1102I–*Not*I fragment containing the 3′ end of the *rfc* coding region fused to the GFP coding sequence was used to replace the 3′ end of the 7 bp deletion construct. The resulting construct was called pMtxR2-4B-GFP.

Subsequently, to maximize fluorescence, the GFP in each construct was exchanged for EGFP. The pMtxR2-4A-EGFP construct contains the *Sph*I–*Eco*RI fragment from pMtxR2-4A-GFP in a wild-type hamster *rfc* construct with a C-terminal EGFP fusion (pMtxT9-EGFP). A *Bam*HI–*Not*I fragment encompassing GFP in the pMtxR2-4B-GFP construct was replaced by a similar fragment from pEGFP-N1 resulting in pMtxR2-4B-EGFP. All constructs were sequenced for confirmation.

Northern blotting

Poly(A)$^+$ RNA (≈ 5 μg) was separated on a 1.2 %-agarose gel in formaldehyde buffer as outlined by Sambrook et al. [41], and transferred to Hybond XL membrane by the capillary method as

described. Membranes were probed, washed and exposed to X-ray film as previously described [11].

Fluorescence detection of GFP

To detect the expression of the EGFP tagged proteins, adherent live cells were revealed using an LEP Ltd. fluorescent source with an Omega optical XF22 filter set on a Zeiss Axiovert S100 microscope. Images were captured using a Sony DXC-950 camera linked to Northern Exposure image-integration software. For the pMtxR2 4B-EGFP transfected cells with low levels of fusion-protein expression, the fluorescence signal was integrated to reveal the image.

For confocal microscopy, cells were grown on glass coverslips overnight, fixed in 4% paraformaldehyde for 20 min, and mounted on glass slides. The tracking reagent (brefeldin A BODIPY 558/568 conjugate) was incubated with cells prior to fixing for 30 min at 37 °C, and was used on the basis of manufacturer's reports of a predominant localization to the ER, with some staining of the Golgi. Detection was performed on an LSM410 inverted Zeiss laser scanning microscope with LSM410 software, using a krypton/argon laser and a 63× oil-immersion lens under standard conditions. Further imaging analysis was performed using Corel Photo-Paint8, and Corel Draw8.

FACS

For FACS sorting, transfected cells were suspended in growth medium and analysed using a Beckon Dickenson FACS sorter. Cells exhibiting fluorescence (greater than ten times background) after excitation with light at 488 nm and detection at an emission of 507 nm were collected and cultured under G418 selection until enough were available for analysis.

For FACS analysis, more than 1×10^6 cells were collected and washed twice in PBS. Cells were then fixed for 15 min in 4% paraformaldehyde/PBS, and washed extensively with PBS/1% BSA. Samples were analysed on a Becton–Dickinson FACScan instrument using Cell-Quest 3.1F software. Instrument settings were determined using MtxRII 5-3 cells as a guide for size and background fluorescence.

Western analysis

Total cellular extracts were prepared from approx. 2×10^5 cells by lysis on ice in 60 μl of extraction buffer [50 mM Tris/HCl (pH 8.0)/0.15 M NaCl/0.1% SDS/1% Nonidet P40/0.5% sodium deoxycholate/60 μg/ml PMSF/10 μg/ml leupeptin/10 μg/ml aprotinin/20 μg/ml pepstatin/0.2 mM orthovanadate/5× concentrated protease-inhibitor-cocktail tablets (Boehringer Mannheim)]. After centrifugation at 12000 ***g*** for 2 min at 4 °C, the soluble lysate was separated by SDS/PAGE and electro-blotted on to nitrocellulose membranes. For detection of EGFP fusion proteins, the blots were blocked with 5% skim milk/TBST [20 mM Tris/HCl (pH 7.6)/0.137 M NaCl/0.2% Tween 20], treated with antibodies to GFP (ClonTech), washed, and incubated with peroxidase-labelled anti-rabbit antibody (Amersham Pharmacia Biotech). Detection was carried out by chemiluminescence using the ECL® Western-blotting analysis system supplied by Amersham Pharmacia Biotech. The light emission was recorded on X-ray films.

Analysis of glycosylation

Cell lysates were concentrated by acetone precipitation, gently denatured at 50 °C in 1% SDS/2% β-mercaptoethanol and resuspended in the appropriate buffer. For N-glycosidase F analysis, samples were in a final solution containing 60 mM sodium phosphate, pH 7.0, 1% β-mercaptoethanol, 0.5% Nonidet P40, 10 mM EDTA, 2 mM PMSF with N-glycosidase F (Boehringer Mannheim) added to a final concentration of 30–40 units/ml, and incubated at 37 °C for 18 h. Endoglycosidase H_f (New England Biolabs) digestions were performed according to manufacturer's instructions at 37 °C for 18 h. Samples were separated by SDS/PAGE and analysed by Western-blot analysis as described above.

Membrane preparation

Cells were grown to confluency in a 75 mm² flask ($\approx 1.5 \times 10^7$) in appropriate media. Adherent cells were washed twice with cold TNE [10 mM Tris/HCl (pH 7.5)/10 mM NaCl/10 mM EDTA] on ice, scraped off the surface into TNE plus protease inhibitors [0.3 mM PMSF/0.3× protease inhibitor cocktail (Boehringer Mannheim)], and pelleted at 200 ***g*** for 2 min. Pellets were resuspended in ice-cold buffer [10 mM Tris/HCl (pH 7.5)/1 mM $MgCl_2$/0.6 mM PMSF/2.5× protease inhibitor cocktail (Boehringer Mannheim)] and transferred to a pre-cooled Dounce homogenizer. After the cells were disrupted, samples were centrifuged at 500 ***g*** for 5 min and the supernatant centrifuged at 12000 ***g*** for 30 min. The supernatant (soluble fraction) was removed while the membrane pellet was resuspended in TNE plus 30% glycerol and protease inhibitors. Protein levels were quantified using the Bio-Rad protein microassay.

Computer analyses

Computer analyses of the nucleotide sequences were performed using the Genetics Computer Group sequence analysis software package [42].

RESULTS

Identification of mutations in the *rfc* gene in MtxRIIOua^R 2-4 cells

Previously, Northern-blot analysis [11] showed that the mutant MtxRIIOua^R 2-4 cell line, which does not take up or bind Mtx, expressed *rfc* transcripts that were similar in both size and abundance to those present in wild-type cells. Further, these cells can be complemented and regain the ability to take up Mtx by transfection with the cDNA clone pMtxT9 containing the wild-type *rfc* cDNA [11]. This suggests that the *rfc* gene in the MtxRIIOua^R 2-4 cells contains alterations.

To test this, mRNA from the MtxRIIOua^R 2-4 cell line was amplified by RT-PCR and the resulting cDNAs cloned. From the eight clones sequenced, two independent alterations were found, although in no case did both appear in a single clone. These changes did not correlate with the previously described alternatively spliced mRNA variants [20] as both were found in clones of each splice variant. Four of the clones from MtxRIIOua^R 2-4 cells contained a single point mutation at position 1033 where an A nucleotide replaced the G nucleotide of the wild-type *rfc* sequence. This base-pair change leads to the substitution of arginine for the Gly^{345} in the ninth transmembrane domain of the predicted twelve-transmembrane-domain protein structure (Figure 1A). The remaining four clones contained a 7 bp deletion beginning at nucleotide 1152, corresponding to the first base-pair of exon 6. This leads to the loss of two amino acids (residues 385 and 386) as well as a shift in the reading frame resulting in a premature stop codon (Figure 1A). Thus 68 novel amino acids replace the normal 135 amino acids of the wild-type *rfc* open reading frame, leading to a protein with a predicted size of 51.5 kDa.

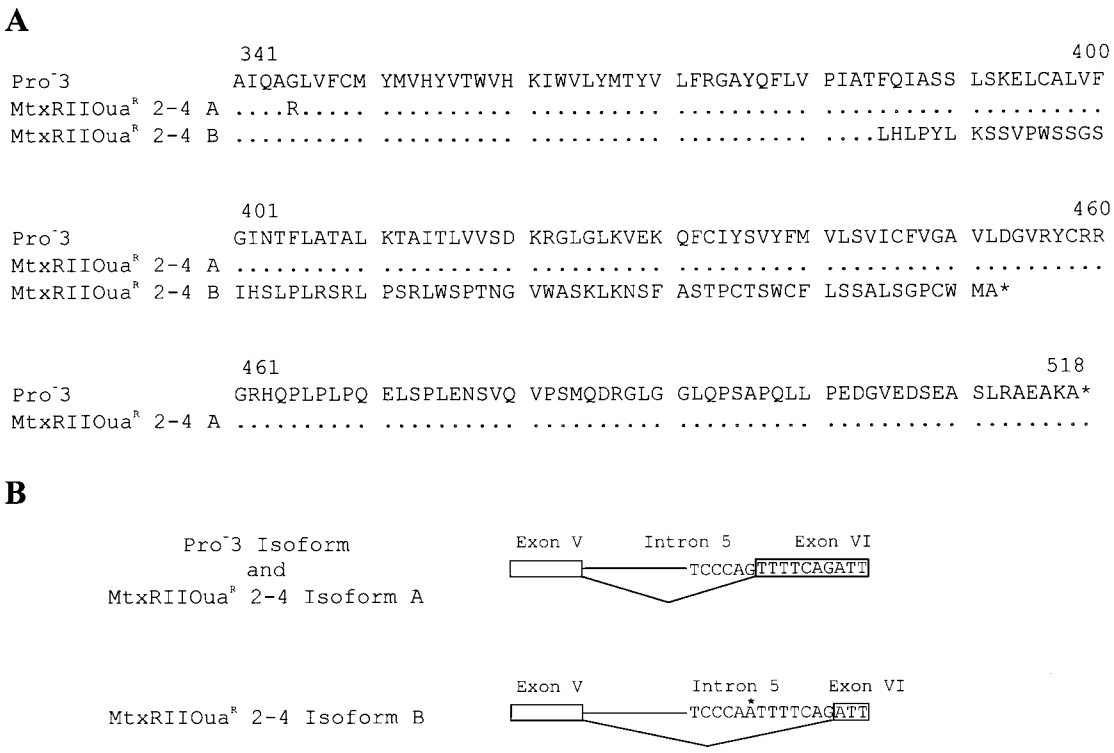

Figure 1 C-terminal amino acid sequence for mutant RFC proteins and mRNA splicing event for isoform B

(**A**) Alignment of the C-terminal amino acid sequences of the *rfc* gene product from Pro^{-}3 and MtxRIIOua^{R} 2-4 cells. The proteins expressed from the two alleles of the *rfc* gene in MtxRIIOua^{R} 2-4 cells are labelled MtxRIIOua^{R} 2-4 A and MtxRIIOua^{R} 2-4 B. Similar amino acids are represented by '.', and non-similar residues are as indicated. The numbers above the sequence indicate the amino acid numbers relative to the previously published hamster *rfc* sequence. The asterisk indicates the termination codon. (**B**) Diagrammatic representation of the splicing event that leads to the seven-base deletion in MtxRIIOua^{R} 2-4 isoform B mRNA.

Six of the eight clones contained additional sequence alterations which were unique to each and were presumed to be polymerase errors introduced during the amplification process.

Confirmation of the mutations in MtxRIIOua^{R} 2-4 cell genomic DNA

To confirm the mutations observed by RT-PCR analysis, these regions were amplified and cycle-sequenced from the genomic DNA of the wild-type Pro^{-}3 and the mutant MtxRIIOua^{R} 2-4 cell lines. The region surrounding the point mutation showed the expected alteration in only one allele of the *rfc* gene from MtxRIIOua^{R} 2-4 cells. At nucleotide position 1033, both a G nucleotide, which corresponded to the wild-type sequence, and an A nucleotide, corresponding to the mutation, were present. This was confirmed by amplifying, cloning and sequencing the appropriate region of the genomic DNA. Of 13 clones from the MtxRIIOua^{R} 2-4 DNA, seven contained an A nucleotide at base-pair 1033 and the remaining six contained a G nucleotide. All eight clones of the Pro^{-}3 DNA contained a G nucleotide at this position. Thus one allele of the *rfc* gene in MtxRIIOua^{R} 2-4 cells contains a point mutation in the coding region.

As previously mentioned, the seven-base deletion begins at the first base of exon 6. Genomic sequencing of this region indicated that the seven bases comprising the deletion in the cDNA were not altered. However, the last base-pair of intron 5 was altered in one allele of the gene, as indicated by a double band (A and G nucleotides) in the DNA sequence. From seven clones of the MtxRIIOua^{R} 2-4 genomic DNA, sequencing indicated that four contained a G nucleotide at the last position in intron 5 and the remaining three had an A nucleotide. All 11 clones from the Pro^{-}3 DNA contained a G nucleotide at this position. Thus the other *rfc* allele in the MtxRIIOua^{R} 2-4 cells contains a point mutation at the AG splice acceptor site of intron 5. The AG dinucleotide that is seven bases into exon 6 acts as an alternate splice acceptor site and leads to a seven-base deletion in the mRNA sequence (Figure 1B).

Functional analysis of the mutant alleles from MtxRIIOua^{R} 2-4 cells

To determine whether these mutations altered the function of the RFC protein, the cDNAs were cloned into an expression vector and transfected into the Mtx-resistant cell line. Selections were carried out in low-folinic acid medium to determine if the mutant constructs could complement the transport deficiency. Neither of the gene products containing the single point mutation (pMtxR2-4A) or the seven-base deletion (pMtxR2-4B) were able to complement the mutant phenotype and allow growth in low levels of folinic acid (Table 1). This is in contrast with the wild-type *rfc* cDNA (pMtxT9), which complemented the mutant cells and restored Mtx-sensitivity, as has been previously reported [11].

Analysis of RFC protein expression

Although the results above indicated that the mutant RFC isoforms are non-functional, it was possible that this was due to

Table 1 Transfection frequencies for phenotypic complementation

DNA source	Number of colonies/10 μg of DNA per 10^6 cells
None	< 0.3
pMtxT9	1580
pMtxR2-4A	< 0.3
pMtxR2-4B	< 0.3
pMtxT9-EGFP	1368
pMtxR2-4A-EGFP	< 0.3
pMtxR2-4B-EGFP	< 0.3

a lack of expression of the protein. Because no antibody to the hamster RFC was available, an EGFP fused to the coding regions of the cDNAs was used to evaluate the mutant translation products in the transfectants. We have recently shown that the EGFP moiety fused in-frame to the human RFC C-terminal serves as a useful reporter for localization without affecting function [26], as does a similar fusion of EGFP to the hamster cDNA. As shown in Table 1, the cDNA (pMtxT9-EGFP) was as effective in complementing MtxRII 5-3 as pMtxT9, indicating that the EGFP fusion does not affect the hamster RFC function. In addition, the kinetic parameters for uptake of Mtx in cells transfected with either the pMtxT9 or pMtxT9-EGFP construct were very similar. Cells transfected with the wild-type construct had an apparent K_t of 1.6 ± 0.6 μM and a V_{max} of 7.6 ± 1.2 pmol/min per mg of protein, while cells transfected with the fusion construct had an apparent K_t of 2.1 ± 0.6 μM and a V_{max} of 5.5 ± 1.2 pmol/min per mg of protein.

To evaluate the expression of the mutant protein isoforms, constructs containing each of the mutant-EGFP and the wild-type fusions were independently transfected into recipient MtxRII 5-3 cells. The transfected cells were selected for the plasmid-encoded neomycin-resistance gene using G418, as there was no selection for fusion-protein expression. Under these conditions, at least 50 % of the cells transfected with the wild-type fusion construct exhibited green fluorescence. In contrast, only 5–10 % of the G418-resistant cells transfected with either pMtxR2-4A-EGFP or pMtxR2-4B-EGFP exhibited fluorescence. Individually selected colonies that exhibited fluorescence were cloned by limiting dilution. RNA blot analysis was carried out on several isolates from each transfection to assess the level of the *rfc* specific message produced (Figure 2). The cells transfected with either pMtxT9-EGFP, pMtxR2-4A-EGFP or the pMtxR2-4B-EGFP constructs produced an *rfc*-specific primary transcript of 2.8 kb in size and a less abundant message at 4.7 kb, with less than two-fold variation among several independently selected isolates. Cells transfected with either pMtxT9-EGFP or pMtxR2-4A-EGFP produced approx. 4-fold more *rfc* transcript than the MtxRIIOua^R 2-4 parental cells, while cells transfected with pMtxR2-4B-EGFP had a slightly lower level of *rfc* message. Thus isolates were FACS-sorted to enrich for those which had high levels of fusion-protein expression, and two independent lines selected in this manner were used in subsequent analyses. As both isolates showed similar properties, representative data is shown for only one independent line. As expected, the transfected cells expressing the pMtxR2-4A-EGFP construct were unable to transport [^{3}H]Mtx at either 37 °C or 30 °C, as were those expressing the pMtxR2-4B-EGFP construct (results not shown).

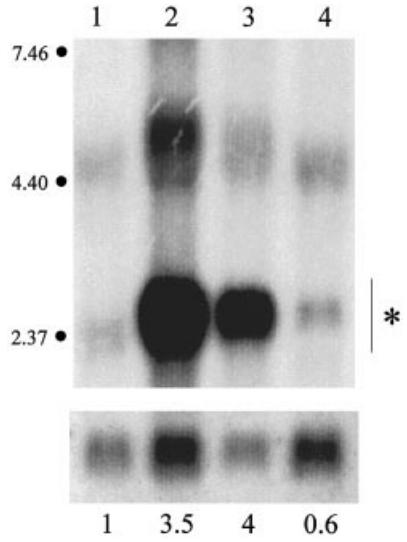

Figure 2 Northern-blot analysis of transfected cells

RNA from representative cell lines stably expressing the fusion constructs was analysed by Northern analysis as in the Experimental section. Lane 1, RNA from parental MtxRIIOua^R 2-4 cells. Lanes 2–4, RNA from cells transfected with pMtxT9-EGFP (lane 2), pMtxR2-4A-EGFP (lane 3) or pMtxR2-4B-EGFP (lane 4). Upper panel, blot probed with *rfc* cDNA; the asterisk indicates primary transcript; lower panel, same blot stripped, and probed with dihydrofolate reductase cDNA. Numbers below indicate the levels of *rfc* message (relative to MtxRIIOua^R 2-4) as standardized by dihydrofolate reductase cDNA abundance. Molecular-mass standards are in kb.

The wild-type RFC–EGFP fusion protein was localized to the cell membrane as indicated by both fluorescence microscopy (Figure 3I) and its predominance in cellular membrane extracts (Figure 4B). Using confocal microscopy it was evident that the majority of the protein was present at the plasma membrane, although a noticeable portion remained intracellular. An overlay of the green EGFP fluorescence with images of a red ER/Golgi stain (Figure 3J–3L) suggests that this intracellular signal (orange) is from protein in the secretory pathway that is likely being processed. This explains the presence of three species in both whole-cell extracts and membrane preparations, where the fusion protein migrates as both a broad band with an apparent molecular size of 95 kDa (Figure 4A), and two less abundant bands at about 75 kDa and 70 kDa. The broadness of the upper band is a reflection of N-glycosylation, as treatment of the protein with N-glycosidase F sharpened the band and decreased its apparent size to approx. 70 kDa (Figure 4C, band C). The middle band (75 kDa, band B) is representative of the core-glycosylated form of the protein, as demonstrated by its sensitivity to endoglycosidase H (Figure 4C), and is likely the form located in the ER. The apparent size of the fully de-glycosylated fusion protein (70 kDa, band C), smaller than the predicted size of 86 kDa, is likely due to incomplete denaturation as the extracts could not be boiled prior to SDS/PAGE because of protein aggregation.

Isolates expressing the pMtxR2-4A-EGFP construct did not show fluorescence at the cellular membrane, but displayed a restricted intracellular signal (Figure 3N). Using confocal microscopy, fusion protein was observed to co-localize with the ER/Golgi-specific stain (Figures 3O–Q) as seen by the overlapping signal (orange). In contrast, the cells expressing the pMtxR2-4B-EGFP construct exhibited a lower level of

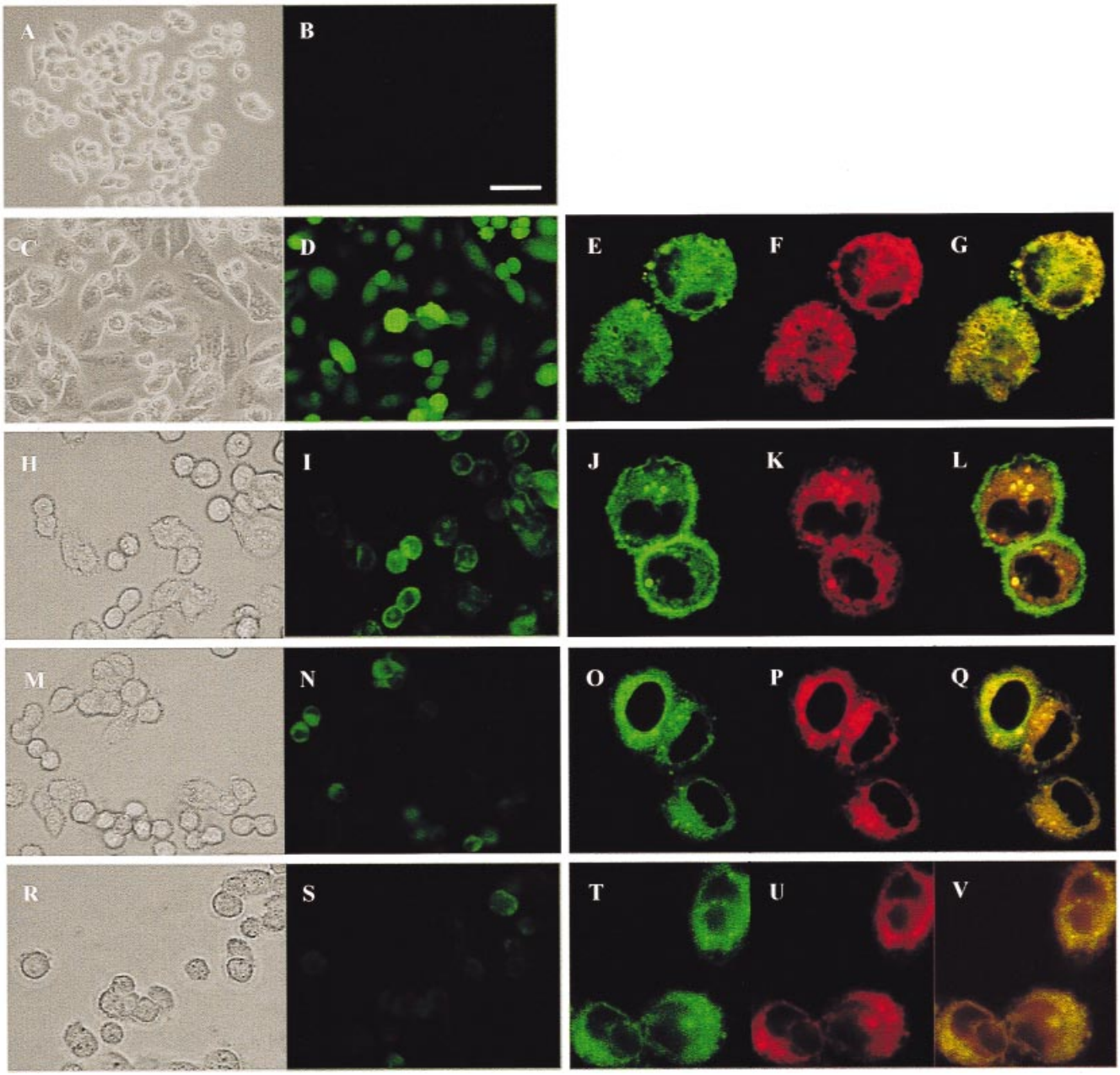

Figure 3 Expression of EGFP fusion proteins

Optical (**A**, **C**, **H**, **M** and **R**) and fluorescence (**B**, **D**, **I**, **N** and **S**) micrographs of MtxRII5-3 cells transfected with various expression plasmids; **E**, **J**, **O** and **T**, confocal images of EGFP fluorescence; **F**, **K**, **P** and **U**, ER/Golgi stained with brefeldin A–BODIPY conjugate; **G**, **L**, **Q** and **V**, overlays of EGFP signal and ER staining; **A**, **B**, untransfected; **C**–**G**, pEGFP-N1; **H**–**L**, pMtxT9-EGFP; **M**–**Q**, pMtxR2-4A-EGFP; and **R**–**V**, pMtxR2-4B-EGFP. The bar represents 50 μm.

fluorescence that did not correlate with the plasma membrane and was both diffuse and punctate in nature (Figure 3S). Using confocal microscopy (Figures 3T–V), it was evident that the splice-mutant RFC protein was distributed in a perinuclear pattern that partially co-localized with the ER/Golgi-specific signal.

In order to confirm the subcellular localization of the expressed mutant fusion proteins, Western blotting was carried out on protein extracts of whole cells and isolated membrane preparations. Cells expressing the pMtxR2-4A-EGFP produced a protein of apparent molecular size 75 kDa (Figure 4A), which remained in the membrane fraction (Figure 4B). The protein product was observed to be sensitive to endoglycosidase H digestion, indicating that only core-glycosylation is present (Figure 4C) and that the protein has failed to progress into the Golgi. The characteristic smear of mature glycosylation is also absent, confirming that the protein processing through the later stages of the secretory pathway is incomplete. Interestingly, significantly more protein was detectable from such cells when they were maintained at 30 °C for 18 h prior to analysis (Figures 4A and 4B). In contrast, cells expressing pMtxR2-4B-EGFP produced very low levels of protein with an approximate mass of

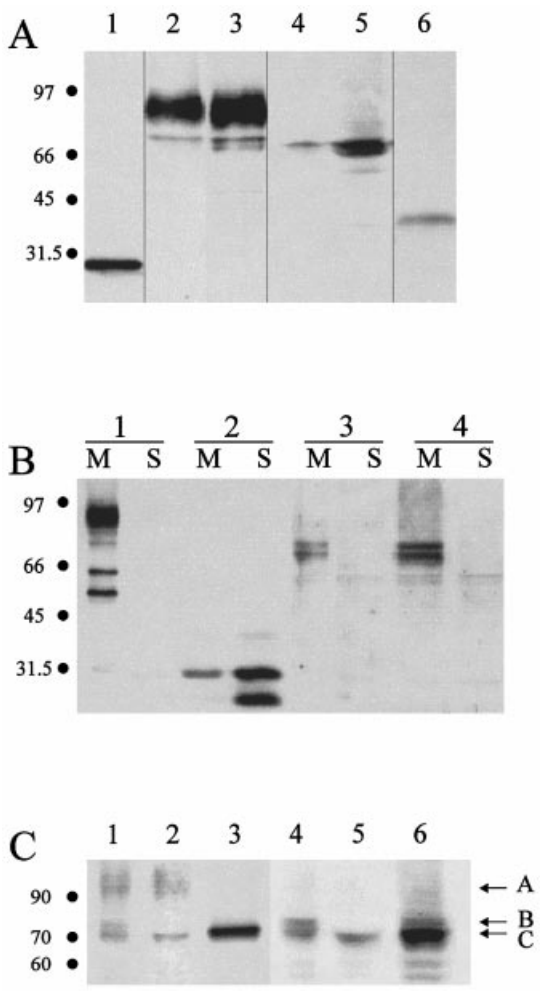

Figure 4 Western-blot analysis of EGFP fusion proteins

(**A**) Extracts were prepared from approx. 2×10^5 stably transfected cell lines maintained at 37 °C (lanes 1, 2, 4 and 6) or at 30 °C, 18 h prior to extraction (lanes 3 and 5). Samples were subjected to SDS/PAGE, electroblotted on to nitrocellulose membranes, and detected using anti-GFP monoclonal primary antibody followed by anti-rabbit secondary antibody conjugated to horseradish peroxidase as described in the Experimental section. Lane 1, cells transfected with pEGFP-N1; lanes 2 and 3, cells transfected with pMtxT9-EGFP; lanes 4 and 5, cells transfected with pMtxR2-4A-EGFP; lane 6, cells transfected with pMtxR2-4B-EGFP. (**B**) Expression of the fusion proteins in crude membrane (M) or cytoplasmic fractions (S). Extracts and membrane fractions were prepared and fusion protein detected as described in Experimental section. Lane 1: M, 2 μg of membrane protein; and S, 2 μg of soluble protein from cells transfected with pMtxT9-EGFP; lane 2: M, 5 μg of membrane protein; and S, 5 μg of soluble protein from cells transfected with pEGFP-N1; lane 3: M, 5 μg of membrane protein; and S, 5 μg of soluble protein from cells transfected with pMtxR2-4A-EGFP maintained at 37 °C; lane 4: M, 5 μg of membrane protein; and S, 5 μg of soluble protein from cells transfected with pMtxR2-4A-EGFP maintained at 30 °C for 18 h prior to the extraction. Lower-molecular-mass products in lane 1M are likely the result of RFC protein degradation during membrane isolation, while that in the soluble GFP sample (lane 2S) is probably material which was fully denatured. The small amount of GFP in the membrane fraction (lane 2M) is likely due to material trapped during sample preparation. (**C**) The total cellular extracts were prepared, treated with endoglycosidase H (lanes 2 and 5), N-glycosidase F (lanes 3 and 6) or not treated (lanes 1 and 4) and analysed as described in the Experimental sexction. Lanes 1–3, 1 μg of extract from cells transfected with pMtxT9-EGFP; lanes 4–6, 50 μg of extract from cells transfected with pMtxR2-4A-EGFP. ← A, mature glycosylated form; ← B, core-glycosylated form; ← C, unglycosylated. In all cases the numbers on the left refer to the protein molecular-size markers in kDa.

36 kDa that did not accumulate when cells were maintained at 30 °C (results not shown). This was true of both isolates examined, although the initial level of fusion protein was variable.

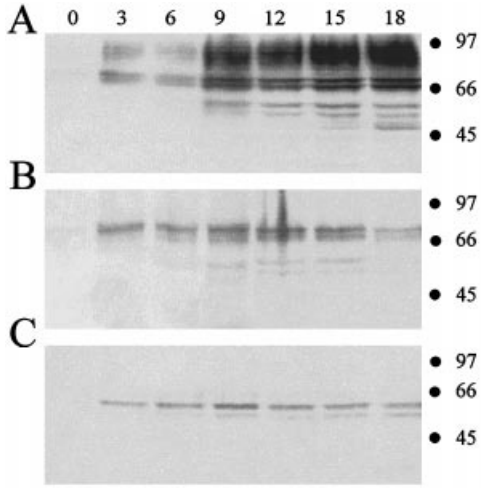

Figure 5 Time course of fusion-protein expression in transiently transfected cells

Individual wells of MtxRII 5-3 cells growing in 24-well tissue culture dishes were transfected with 0.3 μg of construct DNA as described in the Experimental section. At various times after the transfection, cells were harvested from individual wells, extracts prepared, separated by SDS/PAGE, and subjected to Western-blot analysis to detect the fusion protein as described in the Experimental section. (**A**) Cells transfected with pMtxT9-EGFP; (**B**) cells transfected with pMtxR2-4A-EGFP; (**C**) cells transfected with pMtxR2-4B-EGFP. The numbers at the top refer to time (h) post transfection and those on the right to the protein molecular-size markers in kDa.

The protein size was smaller than predicted, but was larger than EGFP alone, suggesting that remnants of RFC were present. Because of the low level of fusion-protein expression in this case, it was difficult to obtain enough material for plasma-membrane preparations, although preliminary results (not shown) indicate that most of the material appears to be in the soluble fraction.

Because of the low expression level of the mutant fusion proteins and the unexpected size of the pMtxR2-4B-EGFP product, transient transfections were carried out to examine the predominant translation product of the constructs. The MtxRII 5-3 cells were transfected with the constructs and, at various times, cellular extracts were prepared and Western-blot analysis carried out (Figure 5). In all cases, the fusion proteins could be detected at 3 h post transfection. For cells transfected with pMtxT9-EGFP, a protein of the expected size (broad band centring around 95 kDa) was shown to increase over the time period of the experiment. For cells transfected with pMtxR2-4A-EGFP, the major product was a doublet of apparent size 75 kDa that is likely the result of incomplete core-glycosylation (see above). There was also a minor doublet around 55 kDa, which matches the pattern in the wild-type lanes, and may represent a degradation product generated during protein turnover. The protein with the point mutation did not accumulate as in the case of the wild-type fusion; rather, expression peaked at about 9–12 h post transfection and subsequently declined. Cells transfected with pMtxR2-4B-EGFP had an expression pattern similar to that for the pMtxR2-4A-EGFP construct where there was little accumulation after 6–9 h. It is noteworthy that whereas the pMtxR2-4B-EGFP product in these transiently transfected cells is larger than in the stably transfected lines (see above), it is still not of the predicted size. However, after long exposures a slightly larger band is evident, and may represent the full-length protein (results not shown).

Protein turnover

The low level of expression of the mutant fusion constructs both in the stably and transiently transfected cells suggested that these proteins may be turned over more rapidly than the wild-type fusion protein. This is supported by the observed accumulation of fusion protein after cells expressing the pMtxR2-4A-EGFP construct are maintained at 30 °C (see above). To examine this, stably transfected cells expressing either pMtxT9-EGFP or pMtxR2-4A-EGFP were grown at either 37 °C or 30 °C for 18 h and then treated with cycloheximide to block protein synthesis. Cellular extracts were prepared at various times and analysed by SDS/PAGE and Western blotting using the α-GFP antibody. As shown in Figure 6, the wild-type fusion protein is relatively stable at both temperatures, showing a slow decrease in abundance. The half-life appeared to be about 24–30 h, but could not be accurately determined, as there was insufficient decline in the protein level over the assay period. In contrast, the point-mutant fusion protein is relatively unstable at both temperatures with a half-life of 1.9 ± 0.1 h and 3.2 ± 0.8 h at 37 °C and 30 °C respectively. It is noteworthy that the lower band representing the unglycosylated forms of the wild-type and mutant protein (Figure 4C, band C), while evident at zero time, rapidly disappeared, as expected, under these conditions.

Involvement of the proteasome

Normal turnover of cellular proteins occurs via targeted degradation by the proteasome [43]. In order to observe whether the observed instability of the point-mutant RFC protein was proteasome-mediated, cells stably expressing either pMtxT9-EGFP or pMtx R2-4A-EGFP were treated with the proteosome-specific inhibitor lactocystin [44], and cellular extracts were examined by Western-blot analysis as shown in Figure 7. Lactocystin treatment of the cells expressing the wild-type fusion protein had little effect upon protein level, although a slight accumulation of the unglycosylated form (70 kDa) was noted. In contrast, treatment of the pMtxR2-4A-EGFP expressing cells resulted in a 2–3-fold increase in the amount of both the core-glycosylated, and unglycosylated forms of the fusion protein, implying that the protein turnover had been inhibited.

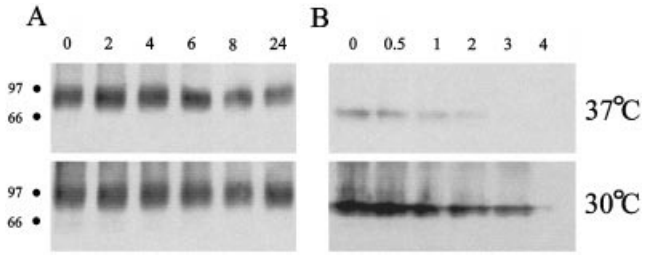

Figure 6 Turnover of fusion proteins

Cell lines stably expressing either pMtxT9-EGFP (**A**) or pMtxR2-4A-EGFP (**B**) were treated with 0.2 mg/ml cycloheximide, cellular extracts prepared and the fusion protein detected by Western blotting as described in the Experimental section. For each time point, extract from approx. 2×10^5 cells was assayed. Cells at 30 °C were maintained at this temperature for 18 h prior to the cycloheximide treatment. Longer exposure times during the detection process indicated the presence of the partially glycosylated forms of the proteins. The numbers at the top of each panel indicate the time (h) when the extracts were prepared post treatment and the numbers on the left indicate the protein molecular-size standards in kDa.

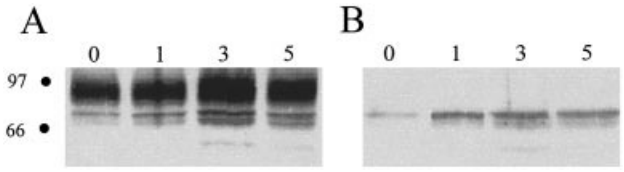

Figure 7 Effect of lactocystin on protein accumulation

Cells stably expressing either pMtxT9-EGFP (**A**) or pMtxR2-4A-EGFP (**B**) were treated with 4 μM lactocystin. Cellular extracts from approx. 2×10^5 cells were prepared for each time point and processed for detection of the fusion proteins as described in the Experimental section. The numbers at the top refer to the time (h) post treatment and the numbers on the left to the protein molecular-size standards in kDa.

DISCUSSION

In the present study we have identified alterations in both alleles of the *rfc* gene in the Mtx-resistant mutant cell line, MtxRIIOua^R 2-4, that reduce stability, interfere with localization and disrupt the function of the encoded protein. This is consistent both with preliminary *in situ* hybridization analysis, which indicates that the *rfc* gene is diploid in this cell line (R. C. Murray, F. P. H. Chan and W. F. Flintoff, unpublished work), and with the recessive mutant phenotype [36], which requires that both alleles must be altered. The recent characterizations of some other Mtx-resistant cell lines have demonstrated that one *rfc* allele carries a mutation, whereas the other is silenced by unknown mechanisms [27,29]. In other systems the situation is more complex, as the gene is present in more than two copies and multiple silencing mechanisms need to occur [30,35]. This characterization of the *rfc* gene in the MtxRIIOua^R 2-4 cell line is the first study where *all* gene products in a Mtx-resistant cell line have been fully examined with respect to their processing and localization.

One mutation that was detected in the MtxRIIOua^R 2-4 *rfc* gene was a single base-pair transition which results in a Gly^{345} → Arg replacement in the ninth transmembrane region. While it is possible that the Gly^{345} is involved in direct binding or translocation of substrate, it is more likely that the large charged side chain of the arginine residue affects the local secondary structure, possibly leading to subtle changes in the overall protein structure. This is consistent with the observation that this glycine residue is conserved within the human, hamster and rat species, and appears as a serine (also a small and not highly charged) residue in the mouse.

Using C-terminal EGFP fusions to monitor protein production, it was demonstrated that the RFC protein containing the point mutation remains trapped in the ER, as both the non-glycosylated and core-glycosylated forms do not appear to progress through the secretory pathway. Furthermore, the half-life of the protein containing the point mutation was dramatically decreased as compared with the wild-type protein. The decrease in turnover rate at 30 °C versus 37 °C may be the result of either a more stable conformation of the point-mutant RFC protein, or a general decrease in the rate of cellular metabolism. However, the former explanation is more consistent with the minor effect of temperature on the wild-type-protein accumulation. The degradation of the point-mutant RFC protein appears to be mediated in part by the proteasome, as lactocystin-based inhibition leads to an accumulation of the ER-retained fusion protein.

A double band on Western blots, centring at approx. 55 kDa, is observed in both the wild-type and the point-mutant RFC protein samples, and may represent an intermediate in the

degradation of the RFC protein. This apparent intermediate is more evident in the transient situation (Figure 5), where the overexpression of the transfected gene may result in a significant portion of protein being diverted down a degradation pathway. The current model for the degradation of membrane proteins involves the cleavage of the polypeptide at various sites to assist in the extraction from the membrane, and then transportation to the proteasome or other degradation machinery [45,46]. Thus these bands may represent the initial degradation product of the RFC protein prior to release to the proteasome, although additional work is necessary to confirm this.

The second point mutation detected in the MtxRIIOua^{R} 2-4 cells leads to the splicing of the pre-mRNA seven bases into intron 5, which shifts the open reading frame and results in an altered C-terminal and premature truncation. Interestingly, the same mutation has been isolated in low abundance from wild-type cDNA [20], although the absence of the mutation in the genomic DNA suggests that this splice acceptor site may normally be inefficient. The detectable protein from the pMtxR2-4B-EGFP fusion was smaller than expected and is present as a soluble and partially degraded form. The effect of the alteration on stability was more difficult to quantify because of insufficient quantities of the fusion protein, although it appears that turnover is also enhanced. There is little accumulation of the mutant product in transiently transfected cells, and the observed size difference between transiently and stably transfected cells implies that this fusion protein is very susceptible to degradation.

An increased rate of protein degradation is a common mechanism whereby cells eliminate mutant proteins [43]. This has been reported for a mutant human RFC protein, where two amino acid alterations dramatically increased the turnover of the protein as compared with the wild-type protein [35]. However, in this situation neither of the individual mutations completely abolished function, suggesting that protein processing was not significantly affected by any one change. In contrast, the single point mutation characterized in the present study is sufficient to interrupt processing, implying that this alteration has a critical effect on the protein folding.

The gene product with the point mutation is strikingly similar to the common cystic-fibrosis-transmembrane-regulator (CFTR) mutant (ΔPhe^{508}) protein, with respect to processing characteristics. Both altered proteins do not appear to proceed beyond the ER, as they are not fully glycosylated, but undergo rapid degradation which is mediated in part by the proteasome [47]. However, while both proteins accumulate at lower temperatures, under these conditions only the CFTR ΔPhe^{508} mutant is able to move through the Golgi to localize at the plasma membrane as a mature and partially functional transporter [48]. These characteristics of the CFTR mutant protein, along with the observations presented in the present study, are suggestive of multiple mechanisms during membrane-protein processing. The rapid degradation of the RFC product with the splice mutation hints at a mechanism which detects significant structural alterations in the overall protein. In contrast, the processing of the RFC product with the point mutation suggests a pathway by which a structurally stable protein can be fully translated and core-glycosylated before degradation. Under certain conditions, partially functional proteins may escape detection and continue through the remainder of the secretory pathway, as in the case of the CFTR ΔPhe^{508} mutant at lower temperatures [48].

While there is considerable information on how proteins are processed in eukaryotic systems, further work is clearly necessary in order to fully appreciate the consequences of single point mutations in large polytopic proteins. The observations made in the present study highlight the need to differentiate between residues that play a role in the overall structure and subsequent intracellular processing, and those which are involved in function.

The present work was supported by a grant from the Medical Research Council of Canada to W.F.F. and a Medical Research Council of Canada Studentship to H.S. We thank R. Tsien for the generous donation of the S65T GFP sequences and T. M. Underhill for the construction of the wild type *rfc* S65T GFP. We thank Martin White for assistance with the FACS analysis and T. M. Underhill for helpful discussions.

REFERENCES

1 Flintoff, W. F. and Nagainis, C. R. (1983) Arch. Biochem. Biophys. **223**, 433–440
2 Goldman, I. D. (1969) J. Biol. Chem. **244**, 3779–3785
3 Goldman, I. D. (1971) Ann. N. Y. Acad. Sci. **186**, 400–422
4 Sirotnak, F. M. (1985) Cancer Res. **45**, 3992–4000
5 Jackson, R. C., Hart, L. I. and Harrap, K. R. (1976) **36**, 1991–1997
6 Galivan, J. (1981) Cancer Res. **41**, 1757–1762
7 Niethammer, D. and Jackson, R. C. (1975) Eur. J. Cancer **11**, 845–854
8 Matherly, L. H., Czajkowski, C. A. and Angeles, S. M. (1991) Cancer Res. **51**, 3420–3426
9 Henderson, G. B. (1986) Folates and Pterins, John Wiley and Sons, New York
10 Gorlick, R., Göker, E., Trippett, T., Waltham, M., Banerjee, D. and Bertino, J. R. (1996) N. Engl. J. Med. **335**, 1041–1048
11 Williams, F. M. R., Murray, R. C., Underhill, T. M. and Flintoff, W. F. (1994) J. Biol. Chem. **269**, 5810–5816
12 Dixon, K. H., Lanpher, B. C., Chiu, J., Kelly, K. and Cowan, K. H. (1994) J. Biol. Chem. **269**, 17–20
13 Williams, F. M. R. and Flintoff, W. F. (1995) J. Biol. Chem. **270**, 2987–2992
14 Said, H. M., Nguyen, T. T., Dyer, D. L., Cowan, K. H. and Rubin, S. A. (1996) Biochim. Biophys. Acta **1281**, 164–172
15 Rubin, S. A., Dyer, D. L., Sharifa, B. G. and Said, H. M. (1995) GenBank℠, Direct Submission, Accession no. U38180
16 Prasad, P. D., Ramamoorthy, S., Leibach, F. H. and Ganapathy, V. (1995) Biochem. Biophys. Res. Commun. **206**, 681–687
17 Moscow, J. A., Gong, M., He, R., Sgagias, M. K., Dixon, K. H., Anzick, S. L., Meltzer, P. S. and Cowan, K. H. (1995) Cancer Res. **55**, 3790–3794
18 Wong, S. C., Proefke, S. A., Bhushan, A. and Matherly, L. H. (1995) J. Biol. Chem. **270**, 17468–17475
19 Nguyen, T. T., Dyer, D. L., Dunning, D. D., Rubin, S. A., Grant, K. E. and Said, H. M.. (1997) Gastroenterology **112**, 783–791
20 Murray, R. C., Williams, F. M. R. and Flintoff, W. F. (1996) J. Biol. Chem. **271**, 19174–19179
21 Tolner, B., Roy, K. and Sirotnak, F. M. (1997) Gene **189**, 1–7
22 Brigle, K. E., Spinella, M. J., Sierra, E. E. and Goldman, I. D. (1997) Biochim. Biophys. Acta **1353**, 191–198
23 Tolner, B., Roy, K. and Sirotnak, F. M. (1998) Gene **211**, 331–341
24 Zhang, L., Wong, S. C. and Matherly, L. H. (1998) Biochem J. **332**, 773–780
25 Williams, F. M. R. and Flintoff, W. F. (1998) Somatic Cell Mol. Genet. **24**, 143–156
26 Ferguson, P. L. and Flintoff, W. F. (1999) J. Biol. Chem. **274**, 16269–16278
27 Brigle, K. E., Spinella, M. J., Sierra, E. E. and Goldman, I. D. (1995) J. Biol. Chem. **270**, 22974–22979
28 Tse, A., Brigle, K., Taylor, S. M. and Moran, R. C. (1998) J. Biol. Chem. **273**, 25953–25960
29 Lefebvre, S. E., Rollins, S. L. and Melera, P. W. (1995) Proc. Am. Assoc. Cancer Res. **36**, 376
30 Gong, M., Yess, J., Connolly, T., Ivy, S. P., Ohnuma, T., Cowan, K. H. and Moscow, J. A. (1997) Blood **89**, 2494–2499
31 Roy, K., Tolner, B., Chiao, J. H. and Sirotnak, F. M. (1998) J. Biol. Chem. **273**, 2526–2531
32 Zhao, R., Assaraf, Y. G. and Goldman, I. D. (1998) J. Biol. Chem. **273**, 7873–7879
33 Zhao, R., Assaraf, Y. G. and Goldman, I. D. (1998) J. Biol. Chem. **273**, 19065–19071
34 Jansen, G., Mauritz, R., Drori, S., Sprecher, H., Kathmann, I., Bunni, M., Priest, D. G., Noordhuis, P., Schornagel, J. H., Piendo, H. M. et al. (1998) J. Biol. Chem. **273**, 30189–30198
35 Wong, S. C., Zhang, L., Witt, T. L., Proefke, S. A., Bhushan, A. and Matherly, L. H. (1999) J. Biol. Chem. **274**, 10388–10394
36 Zhao, R., Sharina, I. G. and Goldman, I. D. (1999) Mol. Pharmacol. **56**, 68–76
37 Flintoff, W. F., Spindler, S. M. and Siminovitch, L. (1976) In Vitro **12**, 749–757
38 Flintoff, W. F., Davidson, S. V. and Siminovitch, L. (1976) Somatic Cell Genet. **2**, 245–261
39 Gross-Bellard, M., Oudet, P. and Chambon, P. (1973) Eur. J. Biochem. **36**, 32–38
40 Underhill, T. M. and Flintoff, W. F. (1989) Somatic Cell Mol. Genet. **15**, 49–59
41 Sambrook, J., Fritsch, E. F. and Maniatis, T. (1989) Molecular Cloning: A Laboratory Manual, 2nd edn., Cold Spring Harbor Laboratory Press, Cold Spring Harbor, NY

42 Genetics Computer Group (1994) Program Manual for the Wisconsin Package, Version 8, Genetics Computer Group, Madison, Wisconsin
43 Jentsch, S. and Schlenker, S. (1995) Cell **82**, 881–884
44 Dick, L. R., Cruikshank, A. A., Destree, A. T., Grenier, L., McCormack, T. A., Melandri, F. D., Nunes, S. L., Palombella, V. J., Parent, L. A., Plamondon, L. and Stein, R. L. (1997) J. Biol. Chem. **272**, 182–188
45 Loo, T. W. and Clarke, D. M. (1998) J. Biol. Chem. **273**, 32373–32376
46 Chang, X. B., Cui, L., Hou, Y. X., Jensen, T. J., Aleksandrov, A. A., Mengos, A. and Riordan, J. R. (1999) Mol. Cell **4**, 137–142
47 Ward, C. L., Omura, S. and Kopito, R. R. (1995) Cell **83**, 121–127
48 Denning, G. M., Anderson, M. P., Amara, J. F., Marshall, J., Smith, A. E. and Welsh, M. J. (1992) Nature (London) **358**, 761–764

Received 21 October 1999/29 November 1999; accepted 22 December 1999